Frustrated Coalescence in a Chemically Reactive Polymer Blend Film

A. Karim,*,† J. F. Douglas,*,† S. K. Satija,† C. C. Han,† and R. J. Goyette‡

National Institute of Standards and Technology, Gaithersburg, Maryland 20899, and Materials Science Division and Intense Pulsed Neutron Source, Argonne National Laboratory, Argonne, Illinois 60439

Received February 26, 1998; Revised Manuscript Received December 21, 1998

ABSTRACT: The phase separation of a thin polymer blend layer undergoing a simultaneous transesterification reaction is examined by a variety of experimental techniques [neutron and X-ray reflectivity, optical microscopy, atomic force microscopy (AFM)] to determine morphological features unique to reactive phase separation. Neutron reflectivity measurements suggest that a copolymer layer reactively forms at the interface between the phase-separating blend components. Evidence for a copolymer layer is also provided by AFM and optical images which indicate a strong inhibition ("frustration") of droplet coalescence and a tendency of the droplets to cluster in late-stage phase separation. The influence of the transesterification reaction on phase separation is found to depend strongly on temperature.

I. Introduction

The phase separation of polymer blends undergoing a simultaneous chemical reaction has recently attracted experimental and theoretical attention.[1−18] Experimental studies have been motivated by the practical problems of controlling the morphology and long-term stability of reactive blends.[1−17] Theoretical motivation for the study of reactive blend phase separation comes from the realization that reaction processes can compete with phase separation leading to qualitative changes in the phase separation process. For instance, steady-state pattern formation can be obtained rather than long-wavelength phase separation under certain circumstances.[18] Previous measurements have shown differences in the phase separation of reactive blends (transesterification) from ordinary blends (see below), but a scientific understanding of these changes is limited. Quantitative measurements of the various stages and morphologies of reactive phase separation are needed to establish the basic phenomenology and relevant parameters controlling reactive blend phase separation. Observations are also required for utilizing reactive blending in a controllable way for technological applications.

Applications involving polymer blends often involve mixing polymers having rather different material properties to obtain some combination of the desirable properties of the blend components. The chemically unlike nature of these materials and the low entropy of mixing of high molecular weight polymers in general makes these mixtures normally rather immiscible so that blending must be achieved by mechanical dispersion rather than thermodynamic mixing. While the initial formation of these dispersions is aided by lowering the interfacial tension between the blend components (an equilibrium "compatibilization effect"), the long-term stability of the dispersion depends strongly on factors influencing the rate of droplet coalescence. Droplet coalescence is often dominated by kinetic parameters such as the surface viscosity of the droplets, and these dynamic compatibilization effects are critical for the long-term stability of the dispersions. Lowering the interfacial tension may help in the dispersal process but may act detrimentally on the long-term dispersion stability by facilitating coalescence. Thus, the ease with which polymer dispersions can be formed and the stability of these dispersions depend on a delicate balance of kinetic and thermodynamic factors.

Emulsification of polymer mixtures through the introduction of copolymers or other surfactant material is an attractive approach to "blend compatibilization", but the typically high viscosity of polymers limits the rate at which the surfactant material finds its way to the interface between the homopolymer fluids. This diffusion-limited process[19] should further lead to a slow evolution in the surface properties of the dispersed particles and thus to changes in blend−surfactant mixture properties over long time scales. The problem of slow surfactant transport can be circumvented by reactively forming interfacially active material *directly* at the interface of the dispersed droplets.

Reactive blending through transesterification[3,6−17] provides an example of this kind of reactive emulsification. A schematic indication of this reaction is given in Figure 1. The homopolymer chains (A, B) form a reactive complex and then disjoin as copolymer chains (A−b−B). In this way the blend *spontaneously generates its own surfactant* to a degree that depends on the rate of reaction (temperature and viscosity dependent). At high temperatures the reaction develops rapidly so that the blend mixture becomes substantially converted into random block copolymer material. In this regime the reaction overwhelms the phase separation process and does not lead to the fine droplet dispersion sought for applications. However, the transesterification reaction leads to more interesting effects at lower temperatures where reaction competes more equally with phase separation.[20] In this regime we can expect the reaction to develop an interfacial layer directly at the surface of the coarsening structures formed during the process of phase separation.

The growth of an interfacially active copolymer layer can be expected to have a large influence on the phase separation of reactive blends. As the transesterification

* To whom correspondence should be addressed.
† National Institute of Standards and Technology.
‡ Argonne National Laboratory.

10.1021/ma980296h This article not subject to U.S. Copyright. Published 1999 by the American Chemical Society
Published on Web 01/29/1999

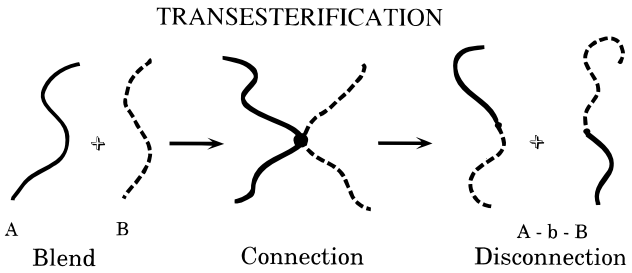

Figure 1. (a) Schematic of transesterification process in a reactive polymer blend. The polymer chains reactively connect and disconnect as copolymers. The process continues, leading to a broad range of molecular weights for the copolymer. (b) Transesterification can lead to direct formation of copolymer at the interface in a phase separated. This has important implications for late stage droplet coalescence, as illustrated in Figure 2.

reaction proceeds, the surfactant concentration increases and the interfacial tension decreases. This effect generally slows down the phase separation process[21,22] and facilitates the breakup of the developing spinodal structure by capillary instability.[23−25] Similar enhanced drop breakup phenomena have been intensively studied in surfactant (e.g., block copolymer) treated blends subject to the complex flow of extruders and other mechanical mixing devices.[26,27] These studies show that *interfacial tension* is a primary parameter in controlling the drop size of the dispersion, especially for low shear rates. Since the threadlike spinodal decomposition pattern is typically rather uniform in the absence of reaction (e.g., ref 28), the droplets formed upon the breakup of this structure should be uniform in size. Indeed, experiments on the breakup of Newtonian liquids threads by capillary instability show that the droplets have remarkably uniform size and shape.[24]

Probably the most important influence of copolymer "compatibilizer" (reactively generated or additive types) on highly immiscible blends is their effect on the kinetics of droplet coalescence.[26] It is appreciated that controlling dispersion stability through control of droplet coalescence is important for diverse applications,[29] but a fundamental understanding of the factors controlling emulsion stability remains elusive.[30] Reactive blends are promising model systems for exploring the physical factors that control emulsion stability since the nature of the copolymer layer can be "tuned" through the extent of chemical reaction.

In the absence of an established theory of emulsion stability and of the factors controlling coalescence of surfactant-coated polymer droplets, some qualitative expectations are worth mentioning for the present study. Consider schematically the primary stages involved in droplet coalescence for regular versus reactive blends. First, long-range hydrodynamic interactions between droplets influence the approach of droplets[31] (See Figure 2). The nature of these forces depends on the viscosity of the surface layer, which in turn influences the frictional drag force on the droplets. Normally, the surfactant increases the drag force so that the encapsulated droplets diffuse more like a hard spheres,[32] even if the droplet viscosity happens to be much lower than the continuous phase. This effect occurs because of inhibited fluid circulation within the droplets as they move, due to the presence of the surfactant layer. Mason and co-workers[24,33] have directly observed this circulation suppression in surfactant-coated drops and explored its consequences on droplet dynamics. They find that

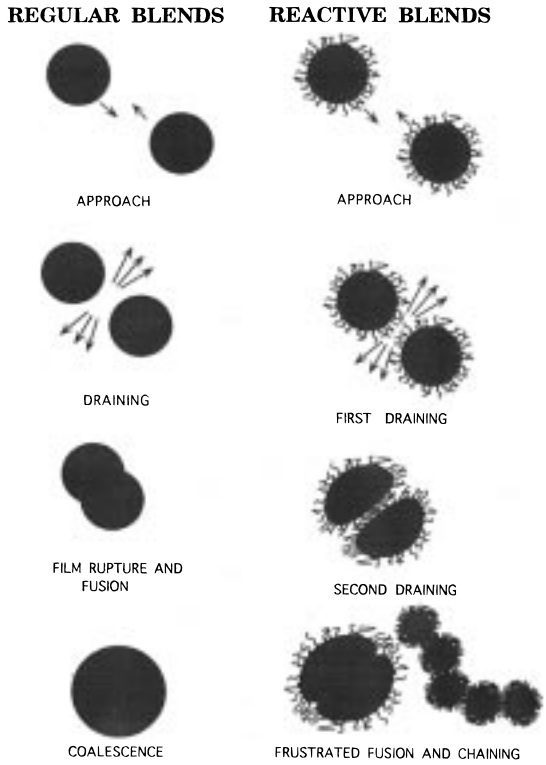

Figure 2. Schematic illustration of droplet coalescence in the usual nonreactive blends compared to one where there is copolymer at the interface. The presence of the copolymer can lead to a "frustration" of the fusion process.

the effect can be very large, sometimes leading to qualitatively different droplet dynamics.

Apart from the influence of the droplet surface coating on the hydrodynamic forces between coated particles, a stronger effect is anticipated in the next stage of coalescence where the coated particles closely approach each other. Before droplet fusion can occur (Figure 2), it is necessary to push out the fluid between the droplet surfaces. Lubrication forces[34] associated with fluid drainage between approaching droplets play a significant role on the rate of droplet coalescence. An order of magnitude estimate of the average time for the draining process to be completed, the "draining time" τ_D , can be obtained from Reynold's lubrication theory,[34]

$$\tau_D \sim \eta R^2 \tag{1}$$

where R is the particle radius and η is the fluid viscosity in the gap between the particles. The instantaneous rate of fluid flow out of the gap depends on the film thickness (droplet boundary assumed to be rigid), but τ_D reflects an average over this evolving gap thickness. Surfactant-coated particles have two draining times τ_{D1} and τ_{D2} associated with the exclusion of the continuous phase between the drops and the exclusion of the surfactant layer coating the droplet. The viscosity of the surfactant layer can be high so that this second drainage process can be rate limiting in the dynamics of droplet coalescence (see below). This second draining stage is complicated by surface tension variations associated with inhomegeneities in the surfactant concentration on the droplet surfaces.[35,36] The gradient in surface tension associated with surfactant concentration gradient tends to promote droplet breakup rather than fusion. Furthermore, Marangoni flows tend to counterbalance

this second draining process and can further inhibit the coalescence process. Thus, the presence of the high-viscosity surfactant layer can be expected to lead to a "frustration" of the droplet coalescence in late-stage phase separation, and significant changes in the late-stage phase separation morphology can be anticipated (see Figure 1).

There is some experimental evidence supporting this simple hydrodynamic model. The contact time required for coalescence of uncoated Newtonian droplets has been found to increase with the continuous phase viscosity and the radius of the coalescing particles.[27] Extensive measurements on the coalescence of surfactant-coated oil drops show that the coalescence time correlates well with the magnitude of the "interfacial viscosity".[37] Wasan et al.[37] discuss many examples where the high interfacial viscosity of coated oil particles (crude oil naturally contains a variety of surfactant molecules) apparently inhibits tertiary oil recovery because of a suppression of droplet coalescence required for extracting oil from the ground. In laboratory experiments on model oil−surfactant emulsions Wasan et al. find that the interfacial tension had *little influence* on their coalescence rate measurements.[37a] We interpret these measurements as implying that the draining time is the rate-limiting step for droplet coalescence in these surfactant-stabilized dispersions. In our view, this kinetic compatibilization effect is the primary factor controlling the long-term stability of reactive blends.

The competition between phase separation and transesterification in immiscible polymer blends of polycarbonate (PC) and deuterated poly(methyl methacrylate) (d-PMMA) has been investigated previously in bulk blends. Rabeony et al.[5] have also studied phase separation in PC−PMMA blends by small-angle light scattering and microscopy. This study revealed an early stage of phase separation that appeared much like ordinary spinodal decomposition, but at later stages the spinodal structure becomes unstable and evolved into a droplet emulsion. Yoon et al.[3,6] utilized small-angle neutron scattering (SANS) and differential scanning calorimetry (DSC) to examine these blends. They found that the global structure coarsens by phase separation for temperatures $T_g < T < 200$ °C, where the glass transition temperature $T_{g,PC}$ is about 150 °C. Transesterification is appreciable at these temperatures, and we interpret our measurements in terms of the formation of copolymer layer about the droplets by transesterification. At higher temperatures ($T > 200$ °C), the initially formed phase-separated structure "dissolves" quickly by the transesterification reaction.

In the present paper we look for more direct evidence of copolymer formation and its effect on late stage coarsening in the reactive PC/d-PMMA blend system. A variety of experimental techniques (X-ray and neutron reflectivity, optical and atomic force microscopy) are used to better quantify features of reactive blend phase separation. The utilization of these techniques requires PMMA deuteration to provide neutron contrast and the preparation of thin blend films to visualize the evolving structures in real space. Measurements are made near and below 200 °C, the temperature where transesterification begins to predominate over phase separation.[3,6,7] These thin-film studies utilize the tendency of phase separation in thin films to cause the surface topography to vary in response to local surface tensions within the film, thus allowing an imaging of the phase separation morphology within the film.[38] Our study focuses on the physical origin of the inhibited coalescence occurring in late stage PC/PMMA blend phase separation. Indirect evidence for the presence of a copolymer layer at the interface between the homopolymer is indicated by neutron reflection measurements on these blend films, while AFM images provide real space images of droplet distortions accompanying the inhibited coalescence of contacting droplets. The kind of droplet distortion[39] seen is similar to observations on foams and emulsions.

II. Experimental Section

Sample Preparation. In the bulk, homogeneous blends of PC/PMMA are difficult to prepare by solvent casting[9] due to the occurrence of phase separation during the solvent evaporation process. Even coprecipitation of the blend followed by pressing and annealing at temperatures around 150 °C typically results in samples that are partially phase separated and transesterified. Rabeony et al.[5] developed a technique for preparing single-phase blend films of PC/PMMA which involves solvent casting from warm (≈40 °C) THF solution. The blend is miscible in this solvent, and the solvent can be evaporated quickly using this method to obtain films that are initially smooth and relatively homogeneous.[40]

Thin-film blend (50:50 by mass) samples of PC (M_w = 34 854; M_w/M_n = 1.7, Aldrich Chemicals)/d-PMMA (M_w= 61 000; M_w/M_n = 1.8, gift from Aristech[41]) were spun-cast at 2000 rpm from warm (≈40 °C) THF solutions onto polished silicon wafers of dimensions 10 cm diameter × 5 mm thick. The wafers were previously cleaned for an hour in a bath of 70% H_2SO_4/30% H_2O_2 (by volume) heated to 80 °C, rinsed thoroughly in deionized water, and dried under flowing N_2 gas. A 1000 Å thick blend film was cast from a 2 mass % solution of the blend while two 490 and 350 Å thick films were coated from more dilute solutions. As cast, the films had a uniform color, indicating a laterally homogeneous mix of the blend components in the plane of the film.[42] All annealing of blend samples was performed under vacuum with maximum annealing temperature of 200 °C. Under these conditions, the homopolymers do not undergo oxidative degradation or cross-linking.

Reflectivity. X-ray reflectivity (XR) measurements were performed on a Scintag instrument[41] equipped with a fixed Cu anode (Kα radiation, λ = 1.54 Å) operated at a power of 1800 KVA. A well-collimated incident beam of X-rays impinged upon the sample surface at a small angle of incidence ($0 < \theta < 5°$), and the specularly reflected beam was picked up by a scintillation detector. Neutron reflection (NR) measurements[43] were made on the as-cast and annealed thin-film blend samples at the BT7 reflectometer at NIST and at the POSY 2 reflectometer at Argonne National laboratory, Illinois. At BT7, neutrons of wavelength $\lambda \cong 2.35$ Å are collimated and reflected from a vertically placed sample, and the reflected beam is picked up by a shielded He^3 pencil detector. The desired q range is attained by changing the angle of incidence (θ) and moving the detector to the 2θ position with respect to the incident beam. Measurements were also performed at the IPNS facility at Argonne National Laboratory, Illinois, on the POSY 2 reflectometer. Briefly, neutrons of wavelength $2 < \lambda < 16$ Å impinge on the sample at fixed angle of incidence and are picked up by the detector. POSY 2 employs a linear position-sensitive detector that can detect off-specular scattering as well. To cover a large q range, measurements are made at more than one angle. Details of the Posy 2 reflectometer and the BT7 reflectometer can be found in refs 44 and 43, 45, respectively.

Microscopy. Surface topographies at ambient temperature were obtained with an atomic force microscope (AFM) and the Nanoscope II (Digital Instruments, Inc.),[41] in a contact mode, using a pyrimidal Si_3N_4 tip in air. Regions were scanned from 100 nm to 100 μm with applied forces in the range 10−40 nN. Images were obtained on different areas of the silicon wafer.

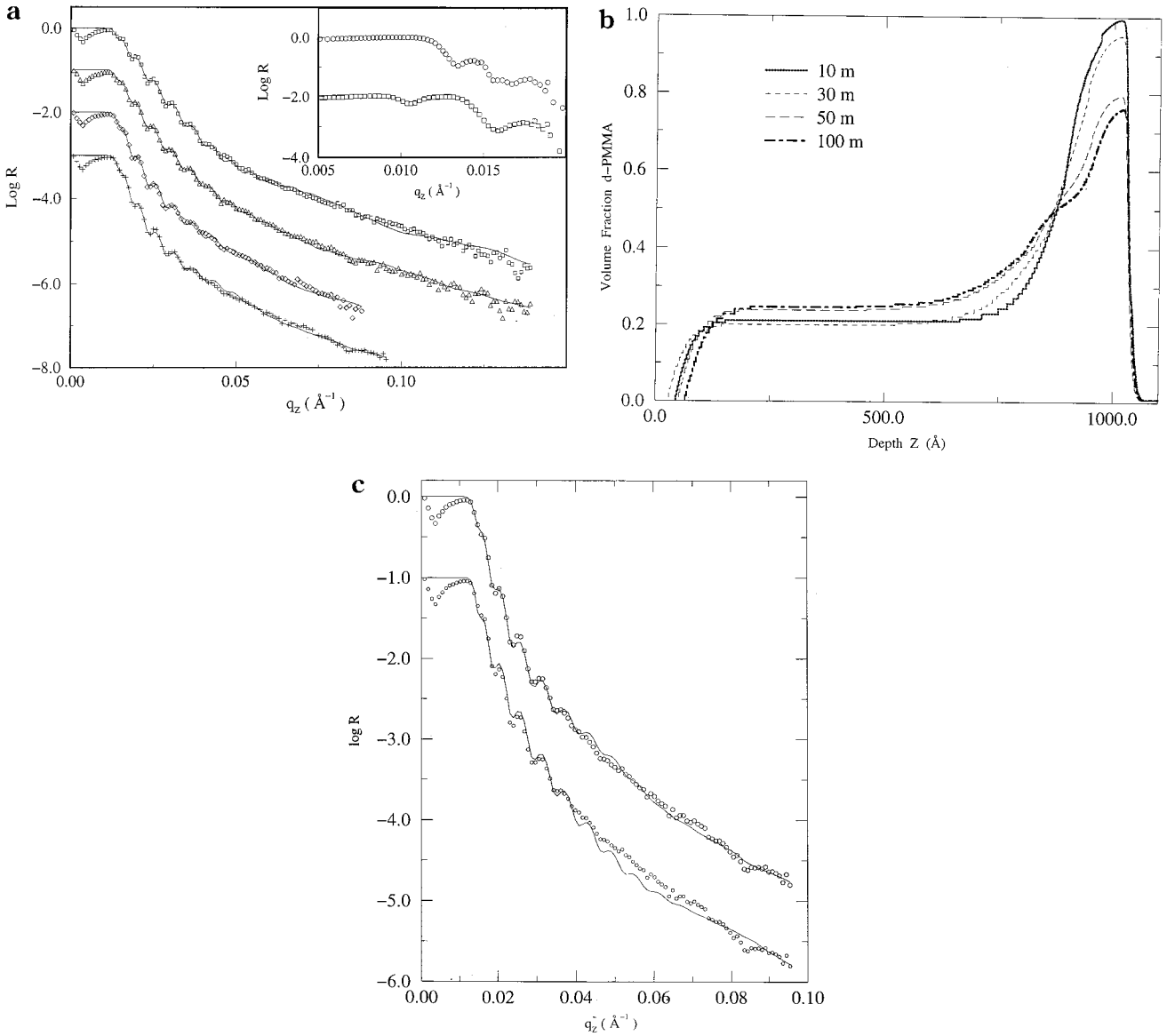

Figure 3. Neutron reflectivity data and composition profiles of reactive blend layers undergoing simultaneous phase separation and transeseterification (T = 180 °C). (a**)** Reflectivities from a PC/d-PMMA spun-cast blend film at different stages of annealing (top to bottom, 10, 30, 50, and 100 min). The solid lines are calculated reflectivities from concentration profiles shown in (b). Inset compares the critical reflecting edge of an as-cast sample versus after annealing for 10 min at 200 °C. An increase of the critical reflecting edge to higher q values indicates a rapid phase separation or layering of the d-PMMA at the silicon wall of the film, necessary for the development of a shoulder in composition profile. (b) Fitted profiles of d-PMMA composition at increasing times in minutes. Note the diminished enrichment of $\phi_{\text{d-PMMA}}$ at the Si surface with increasing time and the development of a shoulder in the composition profile at longer annealing times. (c) Reflectivity comparisons to the 100 min annealed data from profiles with (top fit) and without (bottom fit) the shoulder feature present. The shoulder feature significantly improves the quality of fit.

All AFM images are presented without further processing. Optical micrographs (OM) were obtained using a Nikon reflection optical microscope[41] fitted with a camera, and the pictures were taken at a magnification of 1000×.

III. Results

Section A discusses NR and XR measurements suggesting the formation of a transesterified layer with annealing and associated film surface roughening. Section B focuses on the "late-stage" kinetics and droplet morphology evolution using OM, while section C provides AFM data of the inhibited coalescence phenomena associated with the droplet evolution during very late stage film phase separation.

A. Neutron and X-ray Reflection. Figure 3a depicts a set of neutron reflectivity (NR) data from a film of thickness ≈1000 Å, annealed at 180 °C under vacuum for different periods of time (10, 30, 50, and 100 min). As mentioned before, this temperature was chosen since previous studies[6] have concluded that, above the annealing temperature of ≈200 °C, transesterification reactions compete strongly with phase separation. The solid line fits to the data in Figure 3a are calculated reflectivities based on one-dimensional model density depth profiles shown in Figure 3b for $\phi_{\text{d-PMMA}}$, optimized to best fit the experimental data.[45] (The as-cast composition profiles were difficult to fit, probably due to the nonequilibrium nature of the spin-casting process,[46-48] while it was prevented for t > 100 min due to surface roughness induced by lateral phase separation and chemical reaction.[38,49])

Annealing the film at 180 °C for 10 min has the effect of increasing the critical edge of total reflection com-

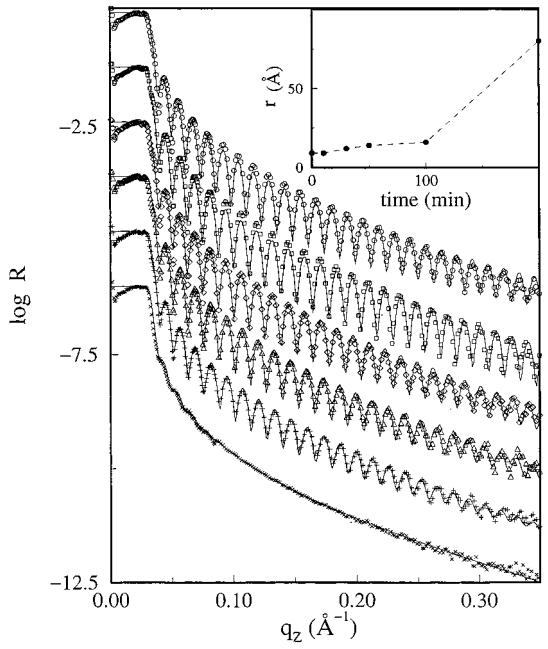

Figure 4. X-ray reflectivity data for a 490 Å reactive blend layer undergoing simultaneous phase separation and transesterification ($T = 200$ °C). Inset denotes the air−film roughness r[51] with increasing annealing time (top to bottom, as-cast, 10, 30, 50, 100, and 200 min). Note that the roughness r increases significantly beyond 100 min.

pared to the as-cast sample, implying a layerlike segregation of d-PMMA within the film. The fit to the 10 min annealed data in Figure 3b shows that the d-PMMA layering occurs near the silicon boundary, with $\phi_{\text{d-PMMA}}$ approaching nearly 95%. Further annealing at 180 °C leads to a decrease of both the d-PMMA volume fraction and thickness near the silicon surface rather than an equilibration of the composition profile as in ordinary blends. We believe this is a consequence of transesterification reaction between the segregated PMMA layer and the bulk of the film which is rich in PC. This interpretation is supported by the gradual development of a shoulder in the reflectivity composition profiles after annealing at 180 °C for times greater than 30 min. This shoulder is interpreted as reflecting the growth of a copolymer layer between PC and d-PMMA as a result of transesterification. A comparative fit to the data with and without the presence of the shoulder is shown in Figure 3c. The width of this shoulder, which is on the order of ≈150 Å, is taken to be a measure of the thickness of the transesterified layer between the PC and the d-PMMA.

Further investigations of the process by neutron reflectivity are not possible due to a dramatic increase of off-specular scattering of neutrons caused by the development of in-plane inhomogeneities. Figure 4 shows a series of X-ray reflectivity data at different annealing times from a film, ≈490 Å thick annealed at 200 °C. These data quantify the growth of surface roughness in our films. The calculated fits in Figure 4 are based on model depth profiles of constant electron density, since the X-ray contrast between PC and d-PMMA is relatively small compared to the air−blend and the blend−silicon interface.[50,51] The inset shows the air/blend interface roughness initially increasing slowly with annealing time and then developing rapidly in time.[52] The order of magnitude roughness development is similar to that in the NR measurements in a similar annealing time frame.

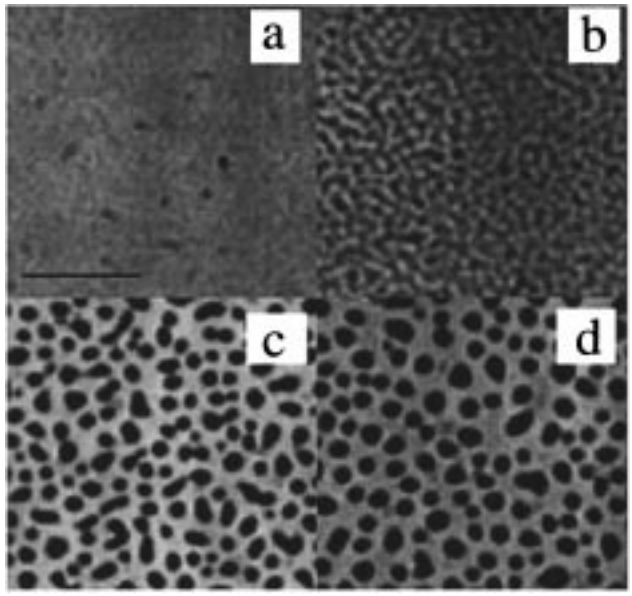

Figure 5. Optical micrograph images (bar = 10 μm) of a 365 Å film annealed at 180 °C for different annealing times, t (min): (a) 30, (b) 60, (c) 300, and (d) 540.

B. Optical Microscopy. All the as-cast samples of thin films blends of PC/d-PMMA were optically clear for the range of film thicknesses studied. We now consider the morphology development by optical microscopy. X-ray reflectivity from a 365 Å thick as-cast film indicated a smooth surface with rms roughness, $r \approx 5$ Å. Optical microscopy (OM) indicated a uniform surface, which was unchanged after annealing for 10 min at 180 °C, suggesting that most of the phase separation at early times occurs in a direction transverse to the film thickness, consistent with the neutron reflection results presented earlier. Upon further annealing for 30 min at 180 °C, the film surface became laterally inhomogeneous, revealing a faint interconnected spinodal decomposition structure (Figure 5a) with a characteristic length scale of ≈0.5 μm. The spinodal pattern is more readily observable in Figure 5b at a longer annealing time of 60 min at 180 °C. A 2-D Fourier transform of the image yields a spinodal ring with a characteristic q^* defining the pattern dimension. Thus, the phase separation process at lower temperatures and early times is not significantly different in reactive versus nonreactive blends.

Figure 5c corresponds to the optical micrograph after the sample was annealed for 120 min at 180 °C. The structure now has a "distorted droplets" morphology. Further annealing for 300 min at 180 °C produced no observable changes either, suggesting a hindered coalescence behavior during the latter stages of phase separation. Only after annealing for 540 min at 180 °C did the droplets shape become more spherical as shown in Figure 5d. The morphology of the distorted droplets is more clearly indicated in AFM measurements presented in section C.

These observations are better quantified by analyzing 2D-FFT's of the OM sequence. Radial averages of these FFT's are shown in Figure 6a. The peak intensity values of q in the radial average of the FFT data are denoted by q^*, and this scale corresponds to the average size of the phase separation pattern. In general, q^* moves to lower q with increasing annealing time, corresponding to an increase in the average size of the structures. This behavior is quantified in Figure 6b, which also indicates

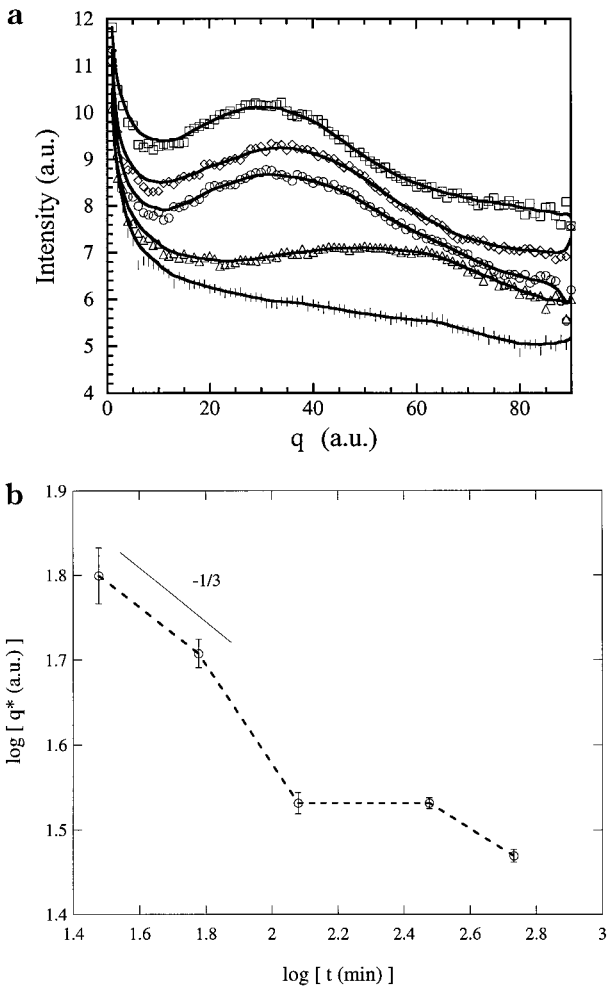

Figure 6. (a) Radial averages of 2D-FFT of the optical micrographs of Figure 5 at $T = 180$ °C. From bottom to top: t (min) = 30, 60, 120, 300, and 540. The peak position of each curve is denoted by q^*. (b) Variation of q^* with annealing time indicates initial conventional phase separation behavior, indicated by a $t^{-1/3}$ behavior, but a plateau at later times is indicative of inhibited coalescence. At still longer times, the droplets coalesce, as shown in the AFM plots of Figure 8.

that the early-stage phase separation follows the $q^* \sim t^{-1/3}$ coarsening found in ordinary blends at early stages of phase separation. Differences between reactive and ordinary phase separation are seen at later times where the droplets become distorted and the coarsening is inhibited. The plateau in Figure 6b may be caused by $\tau_{D2} \gg \tau_{D1}$ (see eq 1). At still longer times, the coarsening process resumes, and we examine later the real space morphology associated with this regime by AFM.

In addition, we performed preliminary measurements at a higher temperature (200 °C) to compare and contrast with the lower temperature measurements. Previous measurements[3,6] in the bulk at this temperature indicated a crossover from a phase separation dominated process to one where the morphological evolution is dictated by transesterification. At 200 °C the droplet dispersion develops rapidly. While the size of the droplets remains roughly constant in time, the number density of droplets increases, and the boundaries of the droplets become increasingly dark and thick in the OM's. At later times the droplets begin to overlap, and the boundaries of the droplets seem to form a "percolating" structure with "chainlike" strands. Figure 7 shows an intermediate stage of this later morphological development in a 1000 Å thick sample that was annealed

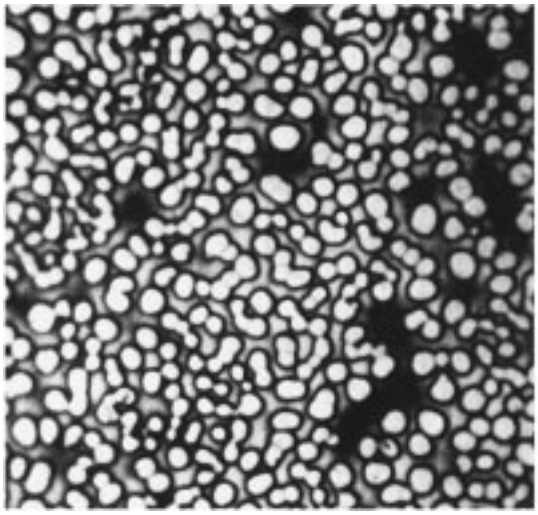

Figure 7. Late-stage phase separation in a 1000 Å reactive blend film at 200 °C. Note the formation of chainlike clusters of droplets. The scale dimensions of the optical micrograph are 57×60 μm.

at 200 °C for several hours. There is a tendency of the coalescing droplets to form small clusters typically involving two or three droplets. This feature, also seen by Rabeony et al.,[5] is a consequence of the free energy (surface area) minimization of the droplets where there is inhibition against droplet coalescence.

C. Atomic Force Microscopy. The three-dimensional surface topologies of some of the thin-film blends of PC/dPMMA were next measured using atomic force microscopy. Figure 8a−d shows AFM micrographs of the 365 Å thick film, and the corresponding optical micrographs are shown in Figure 5. Taking a line profile across the surface of the as-prepared film indicated it to be smooth with rms roughness $r < 5$ Å. These values are in accord with r estimated by X-ray reflectivity on the as-cast film. Figure 8b shows that, after annealing for 60 min at 180 °C, the surface roughening takes the form of a spinodal decomposition like undulation of the free surface of the phase separating blend. A similar phenomenon has been seen in phase-separating thin-film blends of nonreacting polymers.[38] As in previous studies of thin-film phase separation, a 2-D Fourier transform of these surface patterns gives a ring in the intensity distribution at q^* corresponding to the average in-plane scale of the surface pattern. The height scale of the surface undulations (rms roughness of 130 Å) is significant in comparison with the initial film thickness of 365 Å. We note that the relative scale of surface features is considerably more suppressed in thicker films, a feature that was first observed on nonreactive blend films of polystyrene/polybutadiene.[38]

Further annealing up to 300 min leads to the "distorted droplet" morphology seen in the optical micrographs in section B, and the corresponding AFM image is illustrated in Figure 8c. A top view is shown separately in Figure 9. One can see in real space how two initially separated spherical domains have come together and have substantially distorted their shape in an effort to coalesce. The time frame of the hindered coalescence period corresponds to the "plateau region" of Figure 6b, where q^* is nearly invariant. Thus, we surmise that the presence of copolymer around the spherical domains hinders the coalescence process. This result is reminiscent of bulk measurements by Søndergard and Lyngaae-Jørgensen[26a] and Sundaraj and

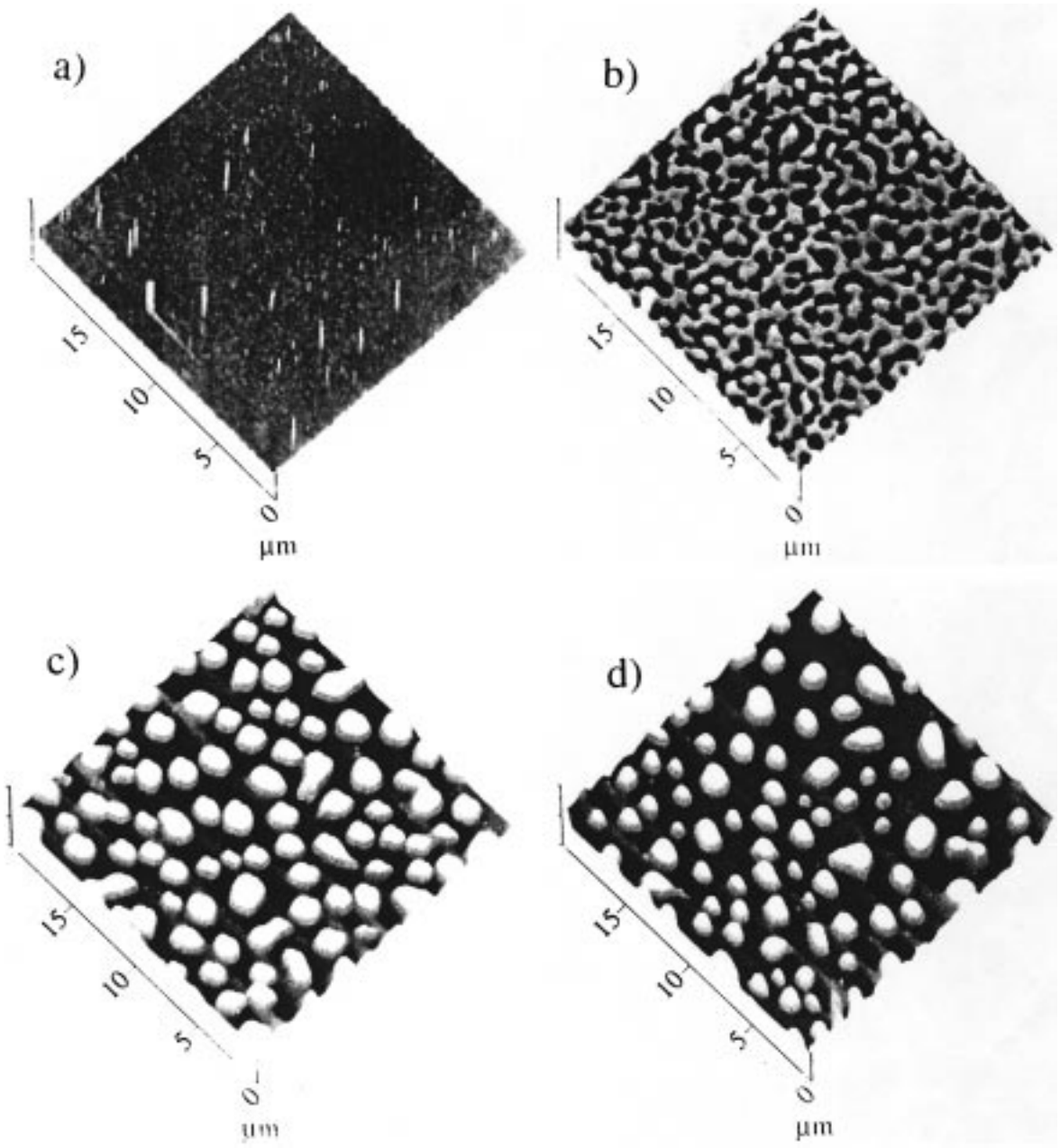

Figure 8. Atomic force microscopy images of phase separation of the thin blend film of Figure 5 undergoing simultaneous transesterification reaction ($T = 180$ °C). (a), (b), (c), and (d) denote the film as-cast, after 60 min, 300 min, and 540 min, respectively. The initial film is (a) homogeneous, and the film in (b) shows a bicontinuous spinodal-decomposition-type pattern in the film height. Inhibited droplet coalescence is apparent in (c), and (d) shows that droplet coalescence ultimately occurs so that inhibition against coalescence is a transient effect in the reactive blend.

Macosko[26b] on the coalescence of dispersed minority phase droplets in a blend with and without the addition of diblock copolymers under steady shear conditions where the block copolymer led to suppressed droplet coalescence. Figure 8d shows that the domains finally coalesce after 540 min of annealing at 180 °C. A line profile for this sample now indicates a peak height of 476 Å for the surface droplets that is even larger than the initial film thickness. Figures 8 and 9 provide direct real-space evidence of inhibited coalescence arising from the presence of the copolymer layer formed in reactive blend phase separation. Such structures are not observed in nonreactive blend films, and it would be interesting to examine block copolymers in highly immiscible blends in the absence of shear to see whether these structures arise in this context. It should be possible to perform more controlled experiments on frustrated phase separation with blend additives since the surfactant can be more readily characterized. Jeon et al.[27] have recently observed droplet clustering in polyolefin films emulsified with block copolymer, and this system might be suitable for studying inhibited coalescence in blend−block copolymer mixtures.

IV. Discussion

The phase separation of the reactive blend polycarbonate (PC) and d-PMMA is found to be significantly different than unreactive blends at temperatures sufficiently high for phase separation and reaction to compete with each other. The transesterification reaction of this blend apparently generates a copolymer material directly at the interface between the blend components that inhibits the coalescence of droplets

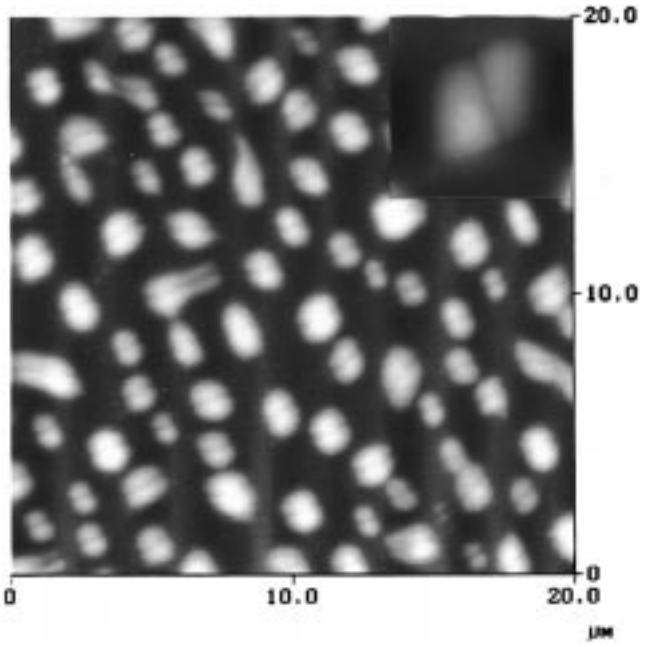

Figure 9. Atomic force microscopy image (top view of Figure 8c) illustrating "frustrated" drop coalescence. Note the formation of "coffee bean"-shaped droplet pairs. An isolated droplet pair is shown in magnified view in the inset at upper right corner.

during the late stage phase separation process. The importance of emulsification effect of this layer on the morphological evolution of phase separation is found in all our measurements. A striking feature of reactive blend is the suppression of spinodal decomposition at long wavelengths. This is a general feature expected for reactive blends when the reaction term competes with phase separation.[18]

An arsenal of tools is utilized to investigate the details of the morphological evolution in reactive blend films. Care was also taken to cast initially uniform blends which were characterized by AFM and X-ray reflectivity. Neutron reflectivity data revealed that the d-PMMA segregated to the Si surface in our thin films and that the films became rough as phase separation and reaction developed. (These features are also found in the phase separation in nonreactive blends.[38]) A novel feature in the reflectivity data is the development of a shoulder in the composition profile of dPMMA (volume fraction) that is interpreted in terms of the development of a copolymer layer formation at the PC/d-PMMA interface.

Optical and AFM microscopy are perhaps the most revealing tools in the present investigation. Samples annealed at 180 °C, where transesterification reaction occurs slowly, show a conventional spinodal decomposition process at earlier stages, but the late stage coalescence of droplets is inhibited. It seems likely this effect is due to copolymer material at the interface of the phase-separating mixture. The AFM exhibits curious "coffee bean"-shaped droplet pairs associated with droplets trying to fuse (Figures 8 and 9). This type of shape minimizes the surface area (free energy) subject to constraint of inhibited fusion and is also seen in soap bubble clusters.[39]

The influence of the transesterification process is more evident in the films annealed at 200 °C. Part of this enhanced effect arises because of the more rapid kinetics, and the phenomena observed appear qualitatively similar to the lower temperature films at longer times. The 200 °C films provide insight into the influence of late stage phase separation with a substantial amount of surfactant.

The following general picture of the morphological evolution emerges: At short times the blend phase separation occurs normally through spinodal decomposition (based on observations by Rabeony et al.[5] that are assumed to apply to our situation), but transesterification inhibits long-wavelength pattern development. The droplets formed through the breakup of the spinodal pattern are nearly monodisperse, and transesterification occurs at the boundary of the droplets leading to a copolymer layer that gradually thickens in time. Ultimately, the droplets evolve to the point where they impinge each other, and the boundary of the droplets forms a percolating structure of the copolymer material. Beyond this point the droplet coalescence is "frustrated" by the layer around the droplets, leading to droplet clustering. At a very late stage of phase separation the coarsening resumes (see Figures 6b and 8d) through intermittent droplet fusion events that trigger large-scale droplet rearrangements (images not shown in the present study). This type of intermittent avalanche-like motion has been observed in simulations of foams.[53] We hope to examine this regime of intermittent droplet coarsening in the future.

Experiments were not performed for $T > 200$ °C. In this case we expect to see the initial formation of droplets which in turn "dissolve" away during the rapid transesterification reaction, and the film should evolve to a homogeneous state. An important question in the case of reactive blends in which the reactive and phase separation effects are balanced is how to control the droplet size in the initial quasi-stationary droplet dispersion. Future experiments should explore the role of small temperature changes, concentration of polymer, polymer molecular weight, and other parameters influencing the size of the resulting droplets. Control of the dispersion morphology in this way should be important for technological applications.

Acknowledgment. We are indebted to Dr. Hichang Yoon for introducing the problem to us. We thank Dr. Gian Felcher and Dr. Apollo Wong for useful discussions related to the neutron reflectivity measurements. We also thank Ferenc Horkay and Eric Amis for useful comments. The work at Argonne was supported by the U.S. Department of Energy, Basic Energy Sciences, under Contract W-31-104-ENG-38.

References and Notes

(1) Okamoto, M.; Inoue, T. *Polym. Eng. Sci.* **1993**, *33*, 175. Yukioka, S.; Inoue, T. *Polymer* **1994**, *35*, 1182.
(2) Guegan, P.; Macosko, C. W.; Ishizone, T.; Hirao, A.; Nakahama, S. *Macromolecules* **1994**, *27*, 4993.
(3) Yoon, H.; Feng, Y.; Qui, Y.; Han, C. C. *J. Polym. Sci., Part B: Polym. Phys.* **1994**, *32*, 1485.
(4) Tamai, T.; Imagawa, A.; Tran-Cong, Q. *Macromolecules* **1994**, *27*, 7486.
(5) Rabeony, M.; Hseih, D. T.; Garner, R. T.; Peifer, D. G. *J. Chem. Phys.* **1992**, *97*, 4505.
(6) Yoon, H.; Han, C. C. *Polym. Eng. Sci.* **1995**, *35*, 1476.
(7) Mijovic, J.; Yee, C. F. W. *Macromolecules* **1994**, *27*, 7287.
(8) Kyu, T.; Lim, D. S. *J. Polym. Sci., Polym. Lett.* **1989**, *27*, 421; *J. Chem. Phys.* **1990**, *92*, 3944, 3951. Kyu, T.; J. M. Saldanha, J. M. *J. Polym. Sci., Polym. Lett.* **1988**, *26*, 33; *Macromolecules* **1987**, *20*, 2840.
(9) Nishimoto, M.; Keskkula, H.; Paul, D. R. *Polymer* **1991**, *32*, 272.
(10) Chiou, J. S.; Barlow, J. W.; Paul, D. R. *J. Polym. Sci., Part B: Polym. Phys.* **1987**, *25*, 1459.

(11) Kim, C. K.; Paul, D. R. *Macromolecules* **1992**, *25*, 3097.
(12) Landry, J. T.; Henrichs, P. M. *Macromolecules* **1989**, *22*, 2157.
(13) Butzbach, G. D.; Wendorff, J. *Polymer* **1991**, *32*, 1155.
(14) Fischer, E. W.; Hellmann, G. P.; Spiess, H. W.; Hörth, F. J.; Ecarius, U.; Wehrle, M. *Makromol. Chem. Suppl.* **1985**, *12*, 189.
(15) Hung, C.-C.; Carson, W. G.; Bohan, S. P. *J. Polym. Sci., Part B: Polym. Phys.* **1994**, *32*, 141.
(16) Debier, D.; Devaux, J.; Legras, R. *J. Polym. Sci., Part A: Polym. Chem.* **1995**, *33*, 407.
(17) Motowoka, M.; Jinnai, H.; Hashimoto, T.; Qui, Y.; Han, C. C. *J. Chem. Phys.* **1993**, *99*, 2095.
(18) Glotzer, S. C.; Stauffer, D.; Jan, N. *Phys. Rev. Lett.* **1994**, *72*, 4109. Glotzer, S. C.; Di Marzio, E. A.; Muthukumar, M. *Phys. Rev. Lett.* **1995**, *74*, 2034. Glotzer, S. C.; Conglio, A. *Phys. Rev. E* **1994**, *50*, 4241. Glotzer, S. C. *Phys. Rev. Lett.* **1994**, *72*, 4109.
(19) (a) Miller, R.; Joos, P.; Fainerman, V. B. *Adv. Colloid Interface Sci.* **1994**, *49*, 249. See references of this paper. (b) Fredrickson, G. H.; Milner, S. T. *Macromolecules* **1996**, *29*, 7386.
(20) We use the term phase separation here to apply to the whole set of dynamical processes by which initially homogeneous fluid mixtures demix. A more precise description distinguishes late-stage coalescence phenomena from the phase separation process at early and intermediate stages.
(21) (a) Laradji, M.; Guo, H.; Grant, M.; Zukermann, M. *J. Phys. A* **1991**, *24*, L629 . (b) Laradji, M.; Mouritsen, O. G.; Toxvaerd, S.; Zukermann, M. J. *Phys. Rev. E* **1994**, *50*, 1243. (c) Yao, J. H.; Laradji, M. *Phys. Rev. E* **1993**, *47*, 2695.
(22) (a) Park, D. W.; Roe, R. J. *Macromolecules* **1991**, *24*, 5324. (b) Izumitani, T.; Hashimoto, T. *Macromolecules* **1994**, *27*, 1744. (c) Sung, L.; Han, C. C. *J. Polym. Sci.* **1995**, *33*, 2405.
(23) (a) Siggia, E. D. *Phys. Rev. A* **1979**, *20*, 595. (b) Mc Master, L. P. *Adv. Chem. Ser.* **1975**, *142*, 43.
(24) (a) Rumsheidt, F. D.; Mason, S. G. *J. Colloid Sci.* **1961**, *16*, 210; **1961**, *16*, 238; **1962**, *17*, 260. (b) Nawab, M. A.; Mason, S. G. *Trans. Faraday Soc.* **1958**, *54*, 1712.
(25) Tomotika, S. *Proc. R. Soc. London, A* **1935**, *150*, 322; **1936**, *153*, 302.
(26) (a) Søndergaard, K.; Lyngaae-Jørgensen, J. Influence of Interface Modification on Coalescence in Polymer Blends. In *Flow-Induced Structure in Polymers*; Nakatani, A. I., Dadmun, M. D., Eds.; American Chemical Society: Washington, DC, 1995; p 169. (b) Sundararaj, U.; Macosko, C. W. *Macromolecules* **1995**, *28*, 2647.
(27) Jeon, H. S.; Lee, J. H.; Balsara, N. P.; Majumdar, B.; Fetters, L. J.; Faldi, A. *Macromolecules* **1997**, *30*, 973.
(28) Glotzer, S. C. *Annu. Rev. Comput. Phys.* **1995**, *2*, 1.
(29) Lissant, K. J. *Emulsion and Emulsion Technology*; Marcel Dekker: New York, 1974; Vol. 6.
(30) (a) Bibette, J.; Morse, D. C.; Witten, T. A.; Weitz, D. A. *Phys. Rev. Lett.* **1992**, *69*, 2439. (b) Exerowa, D.; Kolarov, T.; Khristov, K. *Colloids Surf.* **1987**, *22*, 171. (c) Janssen, J. J. M.; Boon, A.; Agterof, W. G. M. *AIChE J.* **1994**, *40*, 1929. (d) Woods, D. R.; Burrill, K. A. J. *Electroanal. Chem. Interfacial Electrochem.* **1972**, *37*, 191.
(31) (a) Spielman, L. A. *J. Colloid Interface Sci.* **1970**, *33*, 562. (b) Keh, H. J.; Tseng, Y. K. *AIChE J.* **1992**, *38*, 1881. (c) Chen, S. H.; Keh, H. J. *J. Colloid Interface Sci.* **1995**, *171*, 63.
(32) (a) Wasserman, M. L.; Slattery, J. C. *AIChE J.* **1969**, *15*, 533. (b) Rushton, E.; Davies, G. A. *Int. J. Multiphase Flow* **1983**, *9*, 337.
(33) Bartok, W.; Mason, S. G. *J. Colloid Sci.* **1958**, *13*, 293; **1959**, *14*, 13.
(34) Reynolds, O. *Philos. Trans. R. Soc. London, A* **1886**, *177*, 157.
(35) Sonin, A. A.; Bon Fillon, A.; Langevin, D. *J. Colloid Interface Sci.* **1994**, *162*, 323.
(36) (a) Greenspan, H. P. *J. Theor. Biol.* **1978**, *70*, 125. (b) Nir, A. *Phys. Fluids A* **1989**, *1*, 101.
(37) (a) Wasan, D. T.; Mc Namara, J. J.; Shah, S. M.; Sampath, K. *J. Rheol.* **1979**, *23*, 181. (b) Wasan, D. T.; Gupta, L.; Vora, M. K. *AIChE J.* **1971**, *17*, 1287.
(38) (a) Sung, L.; Karim, A.; Douglas, J. F.; Han, C. C. *Phys. Rev. Lett.*, **1996**, *76*, 4368. (b) Karim, A.; Slawecki, T. M.; Kumar, S. K.; Russell, T. P.; Satija, S. K.; Han, C. C.; Liu, Y.; Rafailovich, M.; Sokolov, J.; Overney, R. *Macromolecules* **1998**, *31*, 857. (c) Ermi, B. D.; Karim, A.; Douglas, J. F.; *J. Polym. Sci., Part B* **1998**, *36*, 191. (d) Karim, A.; Douglas, J. F.; Sung, L. P.; Ermi, B. D. *APS News* **1997**, *6*, 25. Lateral phase separation should proceed simultaneously within the bulk of the film, but at a relatively slower rate. This process leads to strong off-specular scattering at later times. This process is studied below through direct real space images of the films using AFM where it is found that the surface undulates in response to phase separation within the film. These previous studies of spun-cast blend films in which one component enriches both the air and solid substrate (symmetric segregation) have shown evidence for a transient relatively rapid change of the composition profile normal to the substrate after initial film formation and a tendency to roughen in time due to the development of surface undulations accompanying phase separation. Here we are interested how these processes become modified in the reactive blend films. In the early time regime $t \approx 10$ min, there seems to be no detectable difference from ordinary blend phase separation.
(39) (a) Foisy, J.; Alfaro, M.; Brock, J.; Hodges, N.; Zimba, Z. *Pacific J. Math.* **1993**, *159*, 47. Morgan, F. *Pacific J. Math.* **1994**, *165*, 347. (b) Almgren, F. J., Jr.; Taylor, J. E. *Sci. Am.* (July) **1976**, *235*, 82.
(40) PMMA segregation to the silicon oxide surface is well determined (e.g. Russell, T. P. *Mater. Sci. Rep.* **1990**, *5*, 171).
(41) Certain commercial equipment, instruments, and materials are identified in this article in order to adequately specify experimental procedure. Such identification does not imply recommendation or endorsement by NIST, nor does it imply that the materials or equipment identified are necessarily the best available for the purpose. According to ISO 31-8, the term molecular weight has been replaced by "relative molecular mass" M_r. The older, more conventional, notation for number-average (M_n) and weight-average (M_w) molecular weights is utilized in the present paper.
(42) In contrast, films prepared from THF solutions at *room temperature* were inhomogeneous and clearly phase separated laterally.
(43) Russell, T. P. *Mater. Sci. Rep.* **1990**, *5*, 171.
(44) Karim, A.; Arendt, B. H.; Goyette, R. J.; Huang, Y. Y.; Kleb, R.; Felcher, G. P. *Physica B* **1991**, *17*, 173.
(45) Ankner, J. F.; Majkrzak, C. F.; Satija, S. K. *J. Res. NIST* **1993**, *98*, 47.
(46) The as-cast density profiles could not be accurately fit due to contrast problem at the polymer−air interface. We can infer from our attempts at fitting these data that d-PMMA is enriched at the silicon oxide surface which occurs during the spin-casting and film-drying process. Matching the critical edge of total reflection gave a surface composition of 85% at the solid boundary. Previous measurements[40] involving PS−PMMA block copolymer indicate that PMMA preferentially segregates to the silicon oxide surface so that polymer−surface thermodynamic interaction may play a predominant role in this segregation phenomenon.
(47) It is known that crystalline polymers generally tend to stay away from surface due to the high energy of the crystal folds (see ref 48). We conjecture that a low, but finite, crystallinity of the PC may be an additional factor responsible for the initial enhancement of the amorphous d-PMMA to the surfaces. This character may be lost once blended in with an amorphous polymer as obtained by annealing the thin films above the glass transition temperatures of both polymers.
(48) Brant, P.; Karim, A.; Douglas, J. F.; Bates, F. S. *Macromolecules* **1996**, *29*, 5628.
(49) Wong, A.; Karim, A.; Han, C. C. *Physica B* **1996**, *221*, 301.
(50) Walpole, R. E.; Myers, R. H. *Probability and Statistics for Engineers and Scientists;* Macmillan Publishing Co.: New York, 1989. The root-mean-square (rms) roughness is defined by the relation $r = \sqrt{\sum_i [z_i - z]^2/N}$, where $z = (\sum_i z_i)/N$.
(51) Feng, Y.; Weiss, R.; Karim, A.; Han, C. C.; Ankner, J. F.; Peiffer, D. G.; *Macromolecules* **1996**, *29*, 3918.
(52) Changes in roughness at the two (asymmetric) interfaces can be distinguished by the fact that increase of roughness at the air boundary causes more of a damping of oscillations while that at the silicon surface causes a rapid drop in the asymptotic value of the reflectivity. (After the first annealing, the oscillations amplitude in Figure 4 are *less damped* but nevertheless accompanied by a decrease in the asymptotic value of the reflectivity. The transient reduction in damping can be attributed to a coincidental quantitative matching of roughness at the two interfaces.)
(53) (a) Okuzono, T.; Kawasaki, K. *Phys. Rev. E.* **1995**, *51*, 1246. (b) Durian, D. J. *Phys. Rev. Lett.* **1995**, *75*, 4780.

MA980296H